Title

ELECTRON ENERGY LOSS SPECTROSCOPY OF CH3NH2 ADSORBED ON Ni(100), Ni(111), Cr(100), AND CR(111)

Authors

Baca, A.G.
Schulz, M.A.
Shirley, D.A.

Publication Date

1985-02-01

Lawrence Berkeley Laboratory
UNIVERSITY OF CALIFORNIA

Materials & Molecular Research Division

Submitted to The Journal of Chemical Physics

ELECTRON ENERGY LOSS SPECTROSCOPY OF CH_3NH_2 ADSORBED ON Ni(100), Ni(111), Cr(100), and Cr(111)

A.G. Baca, M.A. Schulz, and D.A. Shirley

February 1985

Prepared for the U.S. Department of Energy under Contract DE-AC03-76SF00098

DISCLAIMER

LBL-18670

Electron Energy Loss Spectroscopy of CH_3NH_2 Adsorbed on Ni(100), Ni(111), Cr(100), and Cr(111)

A.G. Baca, M.A. Schulz, and D.A. Shirley

Materials and Molecular Research Division
Lawrence Berkeley Laboratory
and
Department of Chemistry
University of California
Berkeley, California 94720

ABSTRACT

Adsorbed CH_3NH_2 has been studied on Ni(100), Ni(111), Cr(100), and Cr(111) at 300 K using electron energy loss spectroscopy. The vibrational spectra indicate that molecular CH_3NH_2 exists on all four surfaces with bonding through the nitrogen lone pair, although a substantial amount of dissociation also occurs on the chromium surfaces. Approximately one monolayer of surface species is the stable coverage on each surface at 300 K. The possible existence of coadsorbed dissociation products CH_x and NH_x is discussed. The CN stretch is anomalously broad on Ni(100) and Ni(111) but not detectably broadened on Cr(100), indicating a strong sensitivity of this bond to interactions with the Ni surfaces. A multiplicity of sites is indicated on Cr(111) by the breadth of all the peaks. The loss spectra exhibit striking intensity differences, which can be attributed partly to impact scattering and partly to intrinsic differences in the interaction of CH_3NH_2 with the different surfaces. A model explaining the linewidth and intensity differences is proposed.

I INTRODUCTION

A molecule can bond to a surface in such a way that no bonds are broken in the process. Two ways for this to occur are through an existing lone pair of electrons in the molecule of interest or through a rehybridization of a π-bonded system. Examples of the former have received much attention, especially the prototype systems CO and NH_3 adsorbed on transition metal surfaces. Adsorption energies tend to be weak (8-17 kcal/mole for NH_3[1-4] and 13-40 kcal/mole for CO[5-13]), making desorption competitive with decomposition on most transition metal surfaces. Molecules such as these provide a known type of interaction, which allows one to examine trends across the periodic table. Examples of π-bonded systems are simple olefins such as ethylene and acetylene, which tend to adsorb more strongly. Their chemistry with transition metals is more reactive. Dissociative chemistry, with the formation of new surface species and/or molecular rearrangements on the surface, is more common than thermal desorption of the parent compound. By attaching a hydrocarbon tail to a lone pair donating group, one can try to bridge the gap between these two types of behavior. Associative interactions in the hydrocarbon group should raise the adsorption energy of the molecule, allowing one to change the decomposition/desorption characteristics.

With these ideas in mind, we present a study of the adsorption of CH_3NH_2 on surfaces of nickel and chromium. These metal surfaces were chosen to provide a comparison between the right and left members of the transition metal series. The interaction of CO with transition

metals shows progressively more dissociative behavior as one goes left and down across the periodic table[14]. The comparison between Ni and Cr is particularly illuminating because Cr is the most reactive metal yet studied. At 300 K, CO is completely dissociated on the structurally different low-index surfaces of Cr at all coverages[15,16]. On Ni there is no dissociation at steps[17] or on the flat, low-index surfaces up to the desorption temperature of 450 K[18]. The study of CH_3NH_2 on these metal surfaces should strengthen this comparison. Structurally different surfaces have been chosen for each metal to separate differences due to structural and electronic properties.

There have been no previous studies on the adsorption of CH_3NH_2 on clean, well characterized, transition metal surfaces. The only previous studies were done on either dispersed particles[19] or poorly characterized surfaces[20,21].

We have carried out this study using electron energy loss spectroscopy (EELS) to determine the chemical identity of surface species (section III) and, where possible, the orientation or symmetry point group (section IV). Intensity and linewidth differences were also observed, with interpretations given in section IV.

II EXPERIMENTAL

The EELS measurements were taken with a previously described spectrometer[22]. Briefly, the design is based on a double pass hemispherical electron monochromator with 1" mean radius and a single

pass analyzer with 2 1/4" mean radius hemispheres, which is rotatable about two independent axes and covers a solid angle of 2π. The impact energy was chosen to optimize the signal and for these studies ranged between 2.0-2.5 eV. The resolution was typically 50-55 cm^{-1} full width at half maximum (FWHM). The scattering geometry will be indicated separately for each measurement.

The single crystals were cut and polished by standard methods. Both the Ni and Cr crystals were precleaned by Ar ion sputtering. During sputtering, the Ni crystal was cycled between 300 K and 1075 K and the Cr crystal between 300 K and 1175 K. Cycling rids the samples of bulk impurities, carbon and sulfur in the case of Ni and nitrogen in the case of Cr. Between experiments, CH_3NH_2 was cleaned from both samples in the same way. First, the sample was sputtered to remove all but residual amounts of carbon. The sample was then exposed to a small amount of oxygen followed by flashing the crystal (1075 K for Ni, 1175 K for Cr) using an electron beam heater. This treatment was sufficient to clean the Ni surfaces. The Cr surfaces required another brief period of sputtering to remove the oxygen. Surface cleanliness was monitored by Auger spectroscopy using a retarding field analyzer.

Methylamine was prepared by hydrolyzing $CH_3NH_2 \cdot HCl$ (Aldrich, 99+% pure) and liberating gaseous CH_3NH_2 from the solution by adding NaOH. The CH_3NH_2 was then purified by several freeze-pump-thaw cycles. It was introduced into an ultra high vacuum (UHV) chamber (base pressure 2×10^{-10} Torr) by means of an effusive

beam doser which could be directed at the sample. Its purity was checked by saturating the UHV chamber with methylamine and waiting to detect the parent ion $CH_3NH_2^+$ with a residual gas analyzer (Inficon IQ200).

III Results

A. Nickel Surfaces

Figure 1 shows the EEL spectra of CH_3NH_2 on Ni(100) and Ni(111). Methylamine exposed to both surfaces reaches a saturation coverage after which no major changes, other than a gradual decrease in the total signal, are observed in the spectra with further exposure. An assignment of the spectra and a comparison with gas phase IR and Raman spectra as well as matrix isolated CH_3NH_2 and cis-$[Pt(CH_3NH_2)_2Cl_2]$ are made in Table 1. Seven peaks in each spectrum can be correlated with the A' normal modes of molecular CH_3NH_2. The other eight normal modes of gas phase CH_3NH_2 can also be accounted for. Modes that occur in the regions 1400-1500 cm^{-1}, 2900-3000 cm^{-1}, and 3200-3300 cm^{-1} could be too close together to be separately resolved or they could be forbidden by the surface selection rule. The assignments will be discussed further in section IV.

For spectra on both surfaces, an extra feature could be attributed to a CO impurity. Such features are commonly present in EEL spectra reported in the literature because CO has a large dynamic dipole moment and is often present in the residual gas of vacuum

chambers. In the CH_3NH_2 spectra, CO probably also comes from the walls of the beam doser. Long purging times to eliminate this source of CO were used at first but were discontinued after degradation in the performance of the EEL spectrometer was noticed. In any case, the amount of CO present on the surface is much less than the proportionate intensity of its loss feature compared to those of CH_3NH_2, because of the much larger dynamic dipole moment of CO.

On both Ni(100) and Ni(111), the spectra can be adequately accounted for by the presence of molecular CH_3NH_2. There are, however, some differences in the spectra. Shifts in peak positions of the internal modes for the chemisorbed molecule from gas phase values are expected, as are differences in these shifts on surfaces with different geometric structures and electronic properties. For example, the C-N stretch occurs at 1010 cm^{-1} on Ni(111) and 1030 cm^{-1} on Ni(100), compared with 1044 cm^{-1} in the gas phase[23-25]. In fact, there are slight variations in the peak positions of all the normal modes of CH_3NH_2 on the two Ni surfaces.

B. Chromium Surfaces

The EEL spectra of CH_3NH_2 on Cr(111) and Cr(100) are shown in Fig. 2. Again, the spectra shown are for saturation coverage at room temperature. The essential features of the spectra are qualitatively the same as for nickel. Six peaks in the spectra, those near 1000, 1185, 1465, 1595, 2940, and 3300 cm^{-1}, have energies only slightly different from corresponding peaks on the nickel surfaces, and are

assigned to internal normal modes of molecular methylamine. A seventh peak in the nickel spectra, the NH_2 wag, ν_9, may be obscured in the chromium spectra by two very intense features at ~ 500 cm^{-1} which are not present in the nickel spectra. These intense features are very similar to peaks observed for dissociated CO on the two Cr surfaces[15], where Cr-C and Cr-O stretches were found to be degenerate in frequency.

A comparison of CH_3NH_2/Cr(100), a c(2x2) N/Cr(100) surface (~ 1/2 monolayer), and 2 L of CO/Cr(100) (saturation coverage), each at 300 K, is shown in Fig. 3. The Cr-N stretch at 560 cm^{-1} is weaker in intensity than the peak at 520 cm^{-1} in the spectrum of dissociated CO (Cr-C and Cr-O stretches). Auger spectra taken after both EEL spectra were collected show no traces of oxygen. The peak at 510 cm^{-1} in the CH_3NH_2/Cr(100) spectrum is assigned as a Cr-C stretch, and such an intense peak can only come from a substantial quantity of dissociated methylamine on Cr(100). The broad feature centered at ~ 500 cm^{-1} on the CH_3NH_2/Cr(111) surface is also very similar to dissociated CO on Cr(111)[15] and indicates that dissociation of CH_3NH_2 occurs on this surface as well.

There is a peak at ~ 2000 cm^{-1} on Cr(111) which is not observed on any of the other surfaces. This may be due to a small amount of molecular CO. We have previously shown that no amount of dissociated CO passivates the Cr surfaces sufficiently to allow the subsequent adsorption of molecular CO at 300 K on these surfaces[15]. It is conceivable that the combination of carbon, nitrogen, and CH_3NH_2

on Cr(111) stabilizes the adsorption of CO from the residual gas in the vacuum chamber. Alternatively, the peak at ~ 2000 cm^{-1} may be due to an overtone of the CN stretch.

Like the companion spectra on the nickel surfaces, there are shifts in the peak positions of the normal modes of CH_3NH_2 adsorbed on the Cr surfaces when compared to gas phase values. The spectra on the Cr surfaces are shifted slightly compared to spectra on the Ni surfaces. There are also intensity and linewidth differences which will be discussed in section IV. It should be noted that some peaks, such as those at 1000, 1185, 1465, and 1595 cm^{-1} on Cr(100), 730 and 1195 cm^{-1} on Ni(111), and 1220 and 1572 cm^{-1} on Ni(100), have widths equal to the instrumental resolution of ~ 50 cm^{-1}, while most of the other peaks are 80 cm^{-1} or broader at the FWHM.

C. Other Results

In much of the discussion that follows, it will be important to establish that methylamine exists on the surfaces studied as approximately one monolayer at 300 K. Auger spectra collected after EELS measurements show the presence of approximately one monolayer of carbon and nitrogen on all four surfaces. We are well aware that high energy electrons (2 KeV) in the fluxes used (50 μA, 5-10 minutes) could desorb and/or dissociate CH_3NH_2 molecules in an "ice" multilayer, and we do not rely on these measurements. Instead, we make a comparison with the results of other workers who use thermal desorption spectroscopy in conjunction with EELS to distinguish

between adsorption of a monolayer, a second adsorbed layer when it can be distinguished from the first layer, and a multilayer. Table 2 shows the boiling point and the desorption temperatures of a multilayer and a second layer for a number of hydrogen containing polar molecules. The results indicate that, for compounds with a wide range of boiling points, the desorption temperatures of a multilayer and a second layer are well below room temperature under UHV conditions. The same conclusion can be reached for CH_3NH_2 adsorbed on transition metal surfaces.

The EELS data are also inconsistent with a multilayer. For a solid crystalline multilayer, the data of adsorbed CH_3NH_2 should have peaks identical in frequency to those of solid crystalline CH_3NH_2 in Table 1. For a disordered multilayer, the EELS data should show broad unresolvable features as they do for several cases with adsorbate molecules of comparable complexity[26-28].

Finally, an attempt to collect spectra of the deuterated compounds CH_3ND_2, CD_3NH_2, and CD_3ND_2 was made in order to comfirm the assignments of Table 1. It was not successful due to isotopic mixing upon interaction of the deuterated methylamine with residual hydrogen on the walls of the beam doser and/or the main UHV chamber.

IV DISCUSSION

A. Mode Assignments and Molecular Orientation

Mode assignments of the spectra in Figs. 1-2 are given in Table

1. Values for the peaks in the bending region 700-1600 cm^{-1} were determined by visual inspection. The good agreement with gas phase and matrix-isolated CH_3NH_2 makes the assignment of the modes ν_4 and ν_{7-9} straightforward. The breadth of the peak at ~ 1465 cm^{-1} makes the assignment of ν_5, ν_6, and ν_{12} ambiguous. We will not discuss the A" modes ν_{13-15} because results from high resolution IR are ambiguous about the assignment of these modes[30-32]. Values for the NH_2 stretches, ν_1 and ν_{10}, were determined by least squares fitting, but fitting was not attempted for the CH_3 stretching region near ~ 2900 cm^{-1} because of its complexity. The gas phase values for ν_2, ν_3 and ν_{11} are listed in Figs. 1-2 and Table 1 as a guide for the reader.

Gas phase CH_3NH_2 belongs to the C_s symmetry point group. Nine of the fifteen vibrational normal modes belong to the totally symmetric representation, A', while six other normal modes belong to the A" representation. Adsorbed CH_3NH_2 can also have C_s symmetry if the plane containing the CN bond and bisecting the NH_2 group is perpendicular to the surface, or it can have the lower symmetry of C_1. For the case of C_s symmetry, the surface selection rule requires that only the nine A' modes be dipole allowed[29]. That is, for spectra collected in the specular direction, these nine A' modes should be the most intense. We observe seven peaks which can be accounted for by eight or nine A' modes and two or three A" modes. In section IV D, we show that the three A" modes ν_{10-12} have contributions from impact scattering. If they

derive all of their intensity from impact scattering, the symmetry of surface CH_3NH_2 is C_s, and, if not, the symmetry is C_1. In either case, the good agreement of our spectra with gas phase[23-25] and matrix-isolated CH_3NH_2[30] supports the assignment of molecular CH_3NH_2 on all four of the surfaces that we have studied.

Evidence also exists for bonding through the nitrogen lone pair. If CH_3NH_2 were bonded side-on instead of through the nitrogen lone pair, one would expect the methyl group to come in close proximity to the surface. This would allow formation of a three-centered M-H-C bond which would significantly weaken the C-H bond and lower the activation barrier to dissociation. Two examples of this effect have been reported in the literature. In the first case, the methyl group of toluene shows enhanced dissociation when compared with the phenyl hydrogens of toluene and benzene on Ni(100) and Ni(111)[33]. In the second example, spectroscopic evidence for C-H bond weakening was found using EELS for C_6H_{12} adsorbed on Ni(111) and Pt(111)[34]. In addition to the expected CH stretch at ~ 2900 cm^{-1}, a very broad and intense feature at ~ 2600 cm^{-1}, indicative of a weakened CH bond, was observed. The lack of such a feature in Figures 1 or 2 supports a model in which the adsorbed CH_3NH_2 bonds to the surface through the lone pair, not a surprising conclusion, as this is the commonly accepted orientation for adsorbed ammonia[3,4,35-41]. The lone pair should be directed approximately perpendicular to the surface in order to keep the hydrogens away from the surface. Small variations of the angle between the lone pair and the surface will be

discussed in section IV D.

Careful examination of the CH_3 stretching region shows a very broad peak which is asymmetric to lower values. Spectra between 2500 and 3500 cm^{-1} are shown in Fig. 4. They are plotted on a logarithmic scale to facilitate comparison of peak shapes. The asymmetry cannot be accounted for by three gaussian peaks near the gas phase values and must be attributed to a small amount of hydrogen bonding, but not of the type discussed in the previous paragraph. Lifetime broadening may be contributing to this line shape.

B. Surface Composition

We cannot address the question of molecular fragmentation definitively because of the complexity of the spectra, but we see little, if any, evidence for molecular fragments on Cr(100) and Ni(111), although there may be some on Ni(100) and Cr(111). We might not be able to detect even substantial quantities of NH_2, NH, or CH_2 because peaks attributable to them would probably fall in a region of the spectrum where there are already peaks. NH and NH_2 have yet to be identified on any surface by vibrational spectroscopy, and peaks due to CH_2, previously observed on Ru(001)[42] and Ni(111)[43], are very weak. Surface CH has been identified on a number of surfaces, including Ni(111)[43] and Ni(100)[44], and has vibrational frequencies at ~ 790 cm^{-1} and ~ 3000 cm^{-1}, almost independent of the surface. As CH is very stable on both Ni(111)[43] and Ni(100)[44] at 300 K, we would expect decomposition of CH_3NH_2

on these surfaces to leave CH. From examination of the region near 790 cm^{-1} in Fig. 1, it can be seen that little or no CH is present on our Ni(111) sample, while there may be some on Ni(100). No evidence of CH is seen on either of the Cr surfaces, although, as mentioned previously, evidence for a large quantity of carbon is observed. The peak at ~ 1300 cm^{-1} on Cr(111) may be due to either a molecular fragment which we cannot identify or to surface hydrogen.

C. Linewidths

There are enough differences in the linewidths of the internal modes of CH_3NH_2 on the four different surfaces to warrant a discussion. The broad linewidths on Cr(111) can be explained by the availability of many inequivalent sites on this very open surface. The broad peak at ~ 500 cm^{-1} indicates a variety of adsorption sites of atoms[15]. A distribution of such sites for CH_3NH_2 should inhomogeneously broaden its internal modes. On the other surfaces, the presence of some narrow lines indicates that selective broadening mechanisms are operative.

On Ni(111), the modes at 1010, 1485, 1570, ~ 2960, and ~ 3300 cm^{-1} are broad. The latter two are broad on all surfaces because symmetric and asymmetric modes overlap. The non-dipole modes ν_{10} and ν_{11}, which would normally have no intensity for spectra collected in the specular direction, contribute to these widths because of contributions from impact scattering. The three A' modes ν_4, ν_5, and ν_6 overlap and make the peaks at 1485 and 1570 cm^{-1}

broad and unresolvable. The CN stretch at 1010 cm^{-1} is both separately resolved and broad, unlike the peaks at 730 cm^{-1} and 1195 cm^{-1}, which have the instrumental FWHM. By repeating the above analysis for the Ni(100) and Cr(100) surfaces, it appears that, on these surfaces, the CN stretch is the only anomalously broad peak. On Ni(100), ν_9 at 770 cm^{-1} may be broad because of overlap with the CH bend, if the CH fragment exists on Ni(100). Alternatively, ν_9 may be anomalously broad on Ni(100) only.

The CN stretch is broader than instrumental resolution on Cr(111), Ni(100), and Ni(111) but narrow on Cr(100). On Ni(100) and Ni(111), some other peaks in the spectrum are narrow. An explanation of these facts necessarily involves an interaction of the CN bond with the Ni surfaces and a waeker interaction between the CH_3 and NH_2 groups and the surface. Such interactions are seen to be plausible by considering the orientation of CH_3NH_2 proposed in section IV A and shown in Fig. 5(a). The CN bond is almost parallel to the surface; a range of CN bond angles could cause differing interactions which inhomogeneously broaden the CN stretch, while keeping hydrogens in the CH_3 and NH_2 groups far enough above the surface to avoid strong interactions that would be observed with our resolution. Reasons for the different bond angles could involve the dynamics of the CN bend or a distribution of slightly different sites, perhaps due to an incommensurate CH_3NH_2 overlayer. Incommensurate overlayers on Ni[46], Pd[47], Pt[48], Co[49], Rh[50], and Ru[51] have been observed for high coverages of CO and should be expected when associative

interactions become competitive with weak, lone pair donor interactions. These ideas are consistent with intensity differences that will be discussed in the next section, and the model will be further developed there.

D. Intensity Differences

There are striking intensity differences between the spectra on the two surfaces. Some of these differences can probably be attributed to the scattering mechanisms of EELS. Impact scattering makes a contribution to the intensities of some of the modes. The angular distribution of impact scattering is relatively flat[45], and its intensity is proportional to the incident electron current. Dipole scattering, on the other hand, is strongly peaked in the specular direction, and the intensity of inelastic features is proportional to the elastically scattered intensity. Any mechanism which lowers the elastic intensity, such as collection at angles other than specular or a decrease in surface order, will lower the intensity of dipole allowed inelastic features but will not change the intensity of the impact scattering features, provided that the incident electron current remains the same. A relative increase in the impact excited peaks is then observed.

Spectra that show enhancement of impact scattering in two ways are shown in Fig. 6. The Ni(100) surface has been exposed to 20 times the saturation exposure of CH_3NH_2, which has the effect of marginally increasing the coverage and inducing disorder, as evidenced

by a fivefold decrease in the count rate of the elastic peak. The spectrum on the Ni(111) surface was collected 15° off specular. When these spectra are compared to those in Fig. 1, a relative increase in the peaks at ~ 1450 cm^{-1}, ~ 2950 cm^{-1}, and ~ 3300 cm^{-1} is seen, which we attribute to the contribution of impact scattering to these peaks.

The remaining intensity differences between the two Ni surfaces are due to intrinsic differences of the interaction of CH_3NH_2 with the each surface. The most significant of these differences involves ν_8, the CN stretch at ~ 1010 cm^{-1}. On Ni(100), the intensity of the CN stretch is approximately a factor of three lower than its intensity on Ni(111) (Fig. 1). The other peaks in the Ni spectra show intrinsic intensities which vary by less than a factor of two relative to other peaks in the same spectrum. On the Cr surfaces, the CN stretch is even more intense relative to the other vibrational modes than it is on the Ni surfaces.

The intensity variations of the CN stretch can be explained on the basis of simple geometrical ideas. Figure 5(a) shows a schematic of surface CH_3NH_2 with the lone pair oriented perpendicular to the surface. The dynamical dipole moment, $d\mu/dr$, of the CN stretch is coaxial with the CN bond and has a normal component proportional to $\sin\theta$ (the parallel component is screened by the surface in dipole scattering). The intensity of a transition is proportional to $\sin^2\theta$, and for small θ, only small changes in θ are required to effect large intensity differences. For the orientation in Fig. 5(a),

θ is approximately 19°, assuming the gas phase geometry for CH_3NH_2. The lower intensity of the CN stretch on Ni(100) can be explained by a value of $\theta \sim 11°$ and the larger intensity on Cr(100) by $\theta \sim 25°$. These orientations are illustrated in Fig. 5(b-d). A larger value of θ on Cr(100) is consistent with a weaker interaction of the CN bond with this surface, as mentioned in the discussion of the narrow linewidth of the CN stretch on Cr(100). These values of θ are proposed to explain why intensity differences occur and are not meant to be structural determinations. On any surface, a range of angles is probably present (as evidenced by broad peaks when the angles are small) and would have to be taken into account before more accurate angular determinations can be made.

Other peak intensities in the spectra are consistent with the above ideas. The symmetric modes ν_3 and ν_6 should show intensity variations like the CN stretch but do not because they overlap with the asymmetric modes ν_2 and ν_5, and also with modes of A" symmetry, ν_{11} and ν_{12}, which gain intensity through impact scattering. The presence of these other overlapping peaks inhibit drastic intensity changes. Much higher resolution would be needed to resolve these peaks and observe intensity variations of individual modes.

When the CN bond angle with the surface is increased on Cr(100), the NH bond angles with the surface are decreased. The amplitude of the NH_2 wag may then be suppressed because of the closer proximity of the NH_2 group to the surface. The lower intensity of the NH_2

wag observed in the spectra on Cr(100) is consistent with this geometry.

E. Comparison Between Ni and Cr

In the introduction, the large differences in reactivity between Ni and Cr surfaces toward CO were mentioned. In the present study, we reach the somewhat surprising conclusion that a substantial quantity of CH_3NH_2 is undissociated on Cr surfaces at 300 K, in contrast to the results for CO, where no undissociated species exist at 300 K. Two possibilities to explain this are as follows: Carbon or nitrogen atoms of initially dissociated CH_3NH_2 can partially passivate the surface and still allow subsequent molecular adsorption, while the presence of oxygen atoms from dissociated CO more totally passivates the surface and would do the same to subsequent exposure to CH_3NH_2. Alternatively, CO could have a lower energy transition state for dissociation, perhaps because of back donation to the π^* orbitals, or perhaps for other reasons. Future experiments to determine the effect of preadsorbed C, N, and O on the adsorption of both CO and CH_3NH_2 would be useful. In a similar study on W(100), a c(2x2)-N overlayer was found to inhibit dissociation of NH_3[52]. The above results point to the possibilities of selective chemistry on W and Cr surfaces, which could someday find new uses in catalysis.

V SUMMARY

A saturation coverage of CH_3NH_2 has been studied on the (100) and (111) surfaces of Ni and Cr at 300 K using EELS. Molecular CH_3NH_2 bonded through the nitrogen lone pair has been identified on each of the above surfaces. On the Cr surfaces, a substantial quantity of dissociation also occurs. CH may be present on Ni(100) but not in substantial amounts on the other surfaces. Other molecular fragments such as CH_2, NH_2, and NH are not detectable by EELS in the presence of CH_3NH_2. The CN stretch is inhomogeneously broadened on the Ni surfaces, and its intensity varies dramatically on the four surfaces. These observations have been explained by a model that takes different CN bond angles with the surface into account.

Acknowledgements

One of us (AGB) gratefully acknowledges financial support from AT&T Bell Laboratories. This work was supported by the Director, Office of Energy Research, Office of Basic Energy Sciences, Chemical Sciences Division of the U.S. Department of Energy under Contract No. DE-AC03-76SF00098.

References

1. J.L. Gland and E.B. Kollin, Surf. Sci. 104, 478 (1981); J.L. Gland and E.B. Kollin, J. Vac. Sci. Technol. 18, 604 (1981).
2. B.A. Sexton and G.E. Mitchell, Surf. Sci. 99, 523 (1980).
3. M. Grunze, F. Bozso, G. Ertl, and M. Weiss, Appl. Surf. Sci. 1, 245 (1978).
4. M. Weiss, G. Ertl, and F. Nitschké, Appl. Surf. Sci. 2, 614 (1979).
5. G. Ertl, Surf. Sci. 47, 86 (1975).
6. D.H. Winicur, J. Hurst, C.A. Becker, and L. Wharton, Surf. Sci. 109, 263 (1981).
7. T.H. Lin and G.A. Somorjai, Surf. Sci. 107, 573 (1981).
8. M.A. Barteau, E.I. Ko, and R.J. Madix, Surf. Sci. 102, 99 (1981).
9. H. Papp, Surf. Sci. 129, 205 (1983).
10. P.A. Thiel, E.D. Williams, J.T. Yates, and W.H. Weinberg, Surf. Sci. 84, 54 (1979).
11. K. Horn, M. Hussain, and J. Pritchard, Surf. Sci. 63, 244 (1977).
12. H. Pfnür, P. Feulner, and D. Menzel, J. Chem. Phys. 79, 4613 (1983).
13. J.N. Allison and W.A. Goddard III, Surf. Sci. 115, 553 (1982).
14. G. Brodén, T.N. Rhodin, C. Brucker, R. Benbow, and Z. Hurych, Surf. Sci. 59, 593 (1976).
15. A.G. Baca, L.E. Klebanoff, M.A. Schulz, E. Paparazzo, and D.A. Shirley, to be submitted to Surface Science.
16. H. Kato, Y. Sakisaka, T. Miyano, K. Kamei, M. Nishijima, and M.

Onchi, Surf. Sci. 114, 96 (1982).

17. E.G. Keim, F. Labohm, O.L.J. Gijzeman, G.A. Bootsma, and J.W. Geus, Surf. Sci. 112, 52 (1981).
18. Z. Murayama, E. Kojima, E. Miyazaki, and I. Yasumore, Surf. Sci. 118, L281 (1982) and references therein.
19. R.W. Sheets and G. Blyholder, J. Catal. 67, 308 (1981).
20. Yung-Fang Yu Yao, J. Phys. Chem. 67, 2055 (1963); Yung-Fang Yu Yao, ibid. 68, 101 (1964).
21. C. Kemball and F.J. Wolf, Trans. Faraday Soc. 51, 1111 (1966).
22. D.H. Rosenblatt, Ph.D. thesis, University of California, Berkeley, 1982 (LBL-14774, unpublished).
23. H. Wolff and L. Ludwig, J. Chem. Phys. 56, 5278 (1972).
24. A.P. Gray and R.C. Lord, J. Chem. Phys. 26, 690 (1957).
25. K. Tamagaka, M. Tsuboi, and A.Y. Hirakawa, J. Chem. Phys. 48, 5536 (1968).
26. S.L. Miles, S.L. Bernasek, and J.L. Gland, Proceedings of the 1982 third International Conference on Vibrations at Surfaces, J. Electron Spectrosc. Related Ph. 29, 239 (1983).
27. K. Christmann and J.E. Demuth, J. Chem. Phys. 76, 6308 (1982).
28. B.A. Sexton, Surf. Sci. 88, 299 (1979).
29. H. Ibach and D.L. Mills, Electron Energy Loss Spectroscopy and Surface Vibrations, (Academic Press, New York, 1982).
30. C.J. Purnell, A.J. Barnes, S. Suzuki, D.F. Ball, and W.J. Orville-Thomas, Chem. Phys. 12, 77 (1976).
31. G.B. Watt, B.B. Hutchinson, and D.S. Klett, J. Am. Chem. Soc. 89,

2007 (1967).

32. J.R. Durig, S.F. Bush, and F.G. Baglin, F. Chem Phys. 49, 2106 (1968).

33. C.M. Friend and E.L. Muetterties, J. Am. Chem. Soc. 103, 773 (1981).

34. J.E. Demuth, H. Ibach, and S. Lehwald, Phys. Rev. Lett. 40, 1044 (1978).

35. F.P. Netzer and T.E. Madey, Surf. Sci. 119, 422 (1982).

36. G.B. Fisher, Chem Phys Lett. 79, 452 (1981).

37. C. Benndorf and T.E. Madey, Skrf. Sci. 135, 164 (1983).

38. T.E. Madey, J.E. Houston, C.W. Seabury, and T.N. Rhodin, J. Vac. Sci. Technol. 18, 476 (1981).

39. R.J. Purtell, R.P. Merrill, C.W. Seabury, and T.N. Rhodin, Phys. Rev. Lett. 44, 1279 (1980); C.W. Seabury, T.N. Rhodin, R.J. Purtell, and R.P. Merrill, Surf. Sci. 93, 117 (1980).

40. G.B. Fisher and G.E. Mitchell, Proceedings of the 1982 third International Conference on Vibrations at Surfaces, J. Electron Spectrosc. Related Ph. 29, 253 (1983).

41. W. Erley and H. Ibach, Surf. Sci. 119, L357 (1982).

42. P.M. George, N.R. Avery, W.H. Weinberg, and F.N. Tebbe, J. Am. Chem. Soc. 105, 1393 (1983).

43. J.E. Demuth and H. Ibach, Surf. Sci. 78, L238 (1978).

44. A.G. Baca, M.A. Schulz, and D.A. Shirley, unpublished results.

45. W. Ho, R.R. Willis, and E.W. Plummer, Phys. Rev. Lett. 40, 1463, (1978).

46. H. Conrad, G. Ertl, J. Küppers, and E.E. Latta, Surf. Sci. 57, 475 (1977).

47. A.M. Bradshaw and F.M. Hoffman, Surf. Sci. 72, 513 (1978).

48. G. Ertl, M. Neumann, and K.M. Streit, Surf. Sci. 64, 393 (1977).

49. M.E. Bridge, C.M. Comrie, and R.M. Lambert, Surf. Sci. 67, 393 (1977).

50. P.A Thiel, E.D. Williams, J.T. Yates Jr., and W.H. Weinberg, Surf. Sci. 84, 54 (1979).

51. E.D. Williams and W.H. Weinberg, Surf. Sci. 82, 93 (1979); G.E. Thomas and W.H. Weinberg, J. Chem. Phys. 70, 1437 (1979).

52. C. Egawa, S. Naito, and K. Tamaru, Surf. Sci. 131, 49 (1983).

Table 1

Vibrational frequencies (cm^{-1}) of CH_3NH_2 in a) the gas phase, b) an argon matrix, c) cis-$[Pt(CH_3NH_2)_2Cl_2]$, d) solid crystalline CH_3NH_2 and adsorbed on e) Ni(100), f) Ni(111), g) Cr(100), and h) Cr(111).

Mode		gas[a]	Ar[b]	cis-$[Pt(CH_3NH_2)_2Cl_2]$[c]	Solid[d]	Ni(100)	Ni(111)	Cr(100)	Cr(111)
A'									
ν_1	NH_2 sym. stretch	3360	3352	3270,3240,3140	3260	3255	3240	3290	3285
ν_2	CH_3 asym. stretch	2962	2967	3016,3000,2952	2899,2881,2865	2960	2960	2960	2960
ν_3	CH_3 sym. stretch	2820	2819	2928,2896	2808,2793	2820	2820	2820	2820
ν_4	NH_2 deformation	1623	1623	1596,1581,1575	1651,1636	1570	1570	1595	1545
ν_5	CH_3 asym. def.	1474	1464	1465,1453	1467	1445	1485	1465	1445
ν_6	CH_3 sym. def.	1430	1450	1429,1417,1405	1441				
ν_7	CH_3 rock	1130	1140	990	1182	1220	1195	1185	1190
ν_8	CN stretch	1044	1052	1037,1017	1048	1030	1010	1000	1020
ν_9	NH_2 wag	780	796	740	955,913	750	730	-	-

Table 1 (continued)

Mode		gas[a]	Ar[b]	cis-$[Pt(CH_3NH_2)_2Cl_2]$[c]	Solid[d]	Ni(100)	Ni(111)	Cr(100)	Cr(111)
A"									
ν_{10}	NH_2 asym. stretch	3424	3415	-	3332,3330	3320	3305	3350	3340
ν_{11}	CH_3 asym. stretch	2985	2991	-	2963,2942,2918	2985	2985	2985	2985
ν_{12}	CH_3 asym. def.	1485	1481	-	1500	-	-	-	-
ν_{13}	NH_2 twist	-	-	-	1353	-	-	-	-
ν_{14}	CH_3 rock	(1195)	-	-	1182	-	-	-	-
ν_{15}	torsion	265	-	-	-	-	-	-	-

a) Refs. 23-25

b) Ref. 30.

c) Ref. 31. The designations A' and A" as well as the mode assignments do not apply.

d) Ref. 32. The designations A' and A" do not apply.

Table 2

The boiling point and desorption temperatures (in degrees Kelvin) of a multilayer are given for a number of polar molecules adsorbed on the indicated surfaces. Where available the desorption temperature of a second adsorbed layer is also indicated.

	boiling point of pure adsorbate	desorption temperature of multilayer	desorption temperature of 2nd layer
H_2S	212	<110[a]	<110[a]
NH_3	240	100-115[b-d]	130-150[b-d]
CH_3NH_2	267	-	-
CH_3OH	338	140-165[e-g]	140-165[e-g]
H_2O	373	150-170[h-l]	180[h]

a) H_2S/Ni(100). A.G. Baca, M.A. Shulz, and D.A. Shirley, J. Chem. Phys. 81, 6304 (1984).

b) NH_3/Ni(111). Ref. 35.

c) NH_3/Pt(111). Ref. 36.

d) NH_3/Ru(001). Ref. 37.

e) CH_3OH/Mo(100), Ref. 26.

f) CH_3OH/Pd(100), Ref. 27.

g) CH_3OH/Pt(111). B.A. Sexton, Surf. Sci. 102, 271 (1981).

Table 2 (continued)

h) H_2O/Ru(001). P.A. Thiel, F.M. Hoffmann, and W.H. Weinberg, J. Chem. Phys. 75, 5556 (1981); T.E. Madey, and J.T. Yates, Jr., Chem. Phys. Lett. 51, 77 (1977).

i) H_2O/Rh(111). J.J. Zinck and W.H. Weinberg, J. Vac. Sci. Technol. 17, 188 (1980).

j) H_2O/Pt(111). G.B. Fisher and J.L. Gland Surf. Sci. 94, 446 (1980).

k) H_2O/Ir(110). T.S. Wittrig, D.E. Ibbotson, and W.H. Weinberg, Surf. Sci. 102, 506 (1981).

l) H_2O/Pt(100). H. Ibach and S. Lehwald, Surf. Sci. 91, 187 (1980).

Figure Captions

Figure 1. EEL spectra for a saturation coverage of CH_3NH_2 on Ni(100) at 300 K. E_o = 2.50 eV, $\theta_i = \theta_s = 45^\circ$. I_o = 44 KHz for Ni(100) and I_o = 58 KHz for Ni(111).

Figure 2. EEL spectra for a saturation coverage of CH_3NH_2 on Cr(100) and Cr(111) at 300 K. E_o = 2.45 eV, $\theta_i = \theta_s = 45^\circ$. I_o = 58 KHz for Cr(100) and I_o = 41 KHz for Cr(111).

Figure 3. EEL spectra of (a) c(2x2)-N/Cr(100) surface, E_o = 2.01 eV, (b) 2.0 L of CO/Cr(100), E_o = 2.12 eV, and (c) a saturation coverage of CH_3NH_2/Cr(100), E_o = 2.45 eV. All spectra were taken at 300 K with $\theta_i = \theta_s = 45^\circ$.

Figure 4. Logarithmic plots of the CH_3 and NH_2 stretching regions for CH_3NH_2 adsorbed on Ni(100), Ni(111), Cr(100), and Cr(111). The lines through the data are the result of a smoothing procedure, not a best fit.

Figure 5. Possible orientations of adsorbed CH_3NH_2 which are consistent with the intensity of the CN stretch on the different surfaces. (a) The nitrogen lone pair is perpendicular to the surface and the CN bond is at an angle θ from the surface. (b) The CN bond is more parallel to the Ni(100) surface, (c) less parallel on Ni(111), and (d) tilted further away on Cr(100). This figure is meant to illustrate orientations of CH_3NH_2 and does not imply site or structure determinations.

Figure 6. Assessing the contribution of impact scattering in the spectra of Fig. 1 by comparing to (a) a Ni(100) surface exposed to 20 times the saturation coverage of CH_3NH_2, E_o = 2.50 eV, $\theta_i = \theta_s = 45^\circ$, I_o = 8.6 KHz and (b) off specular EELS of a saturation coverage of CH_3NH_2/Ni(111) with E_o = 2.50 eV, $\theta_i = 45^\circ$, $\theta_s = 60^\circ$, I_o = 8.6 KHz.

CH_3NH_2: Ni(100), Ni(111)

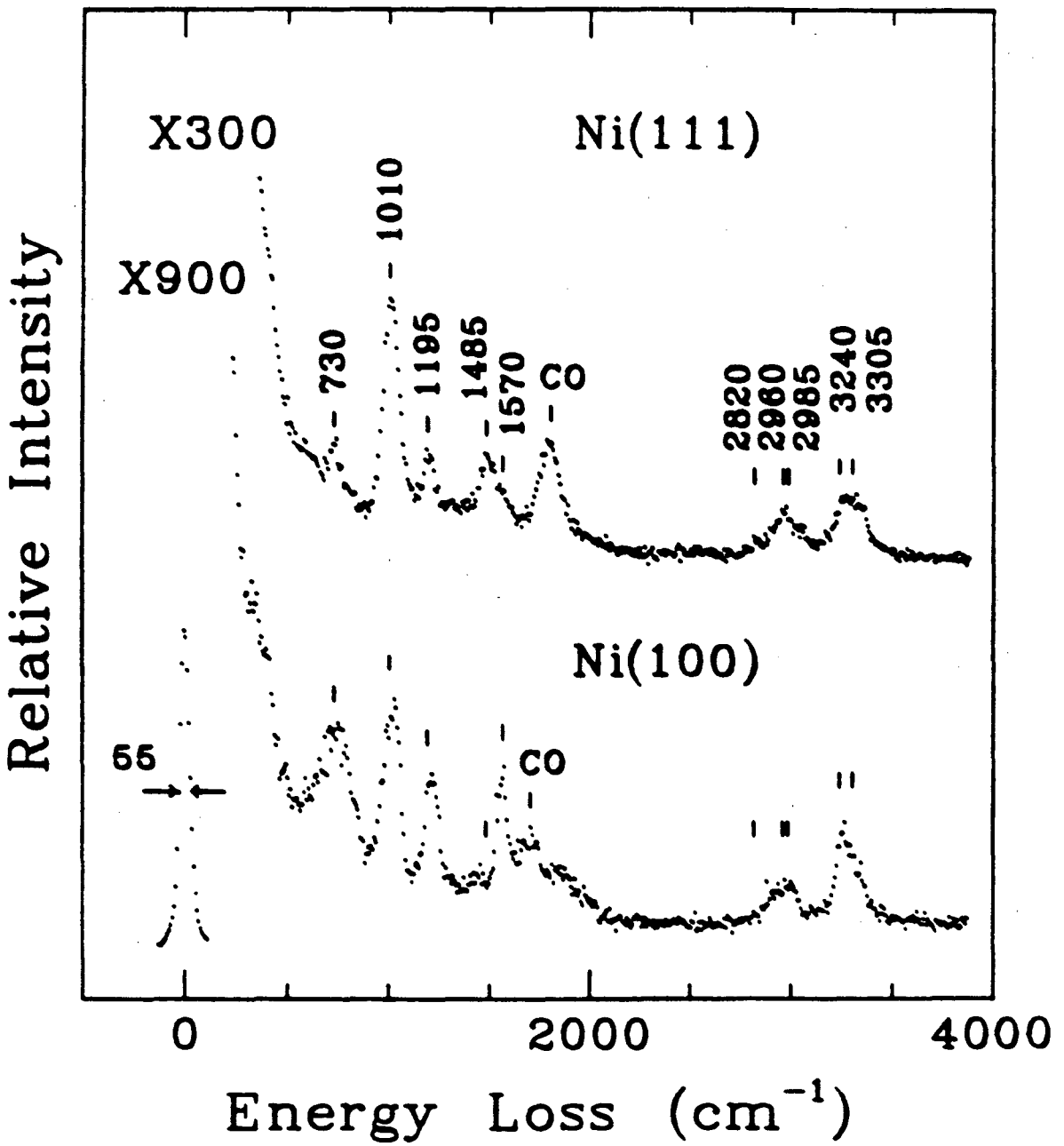

XBL 8412-5206

Figure 1

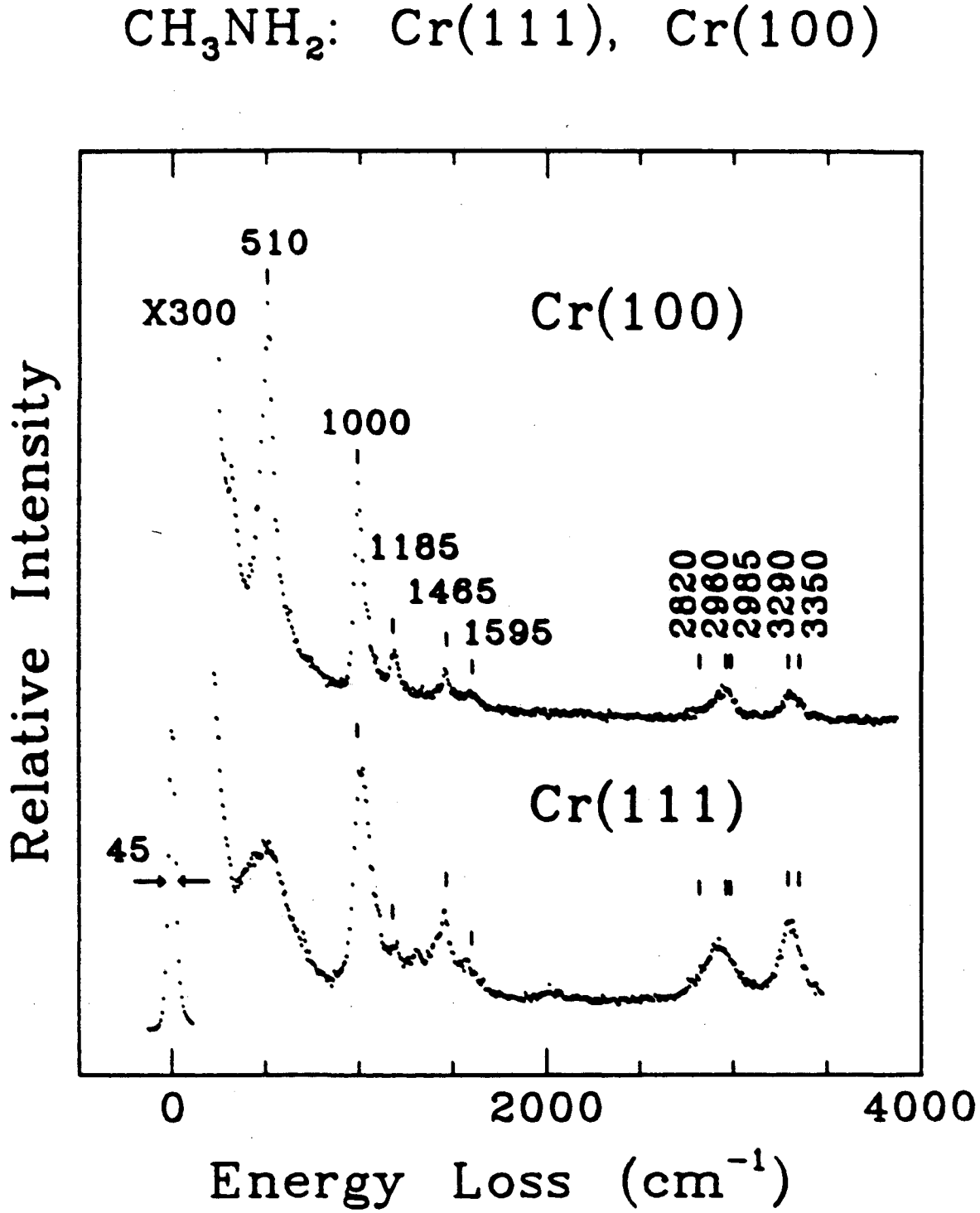

XBL 8412-5208

Figure 2

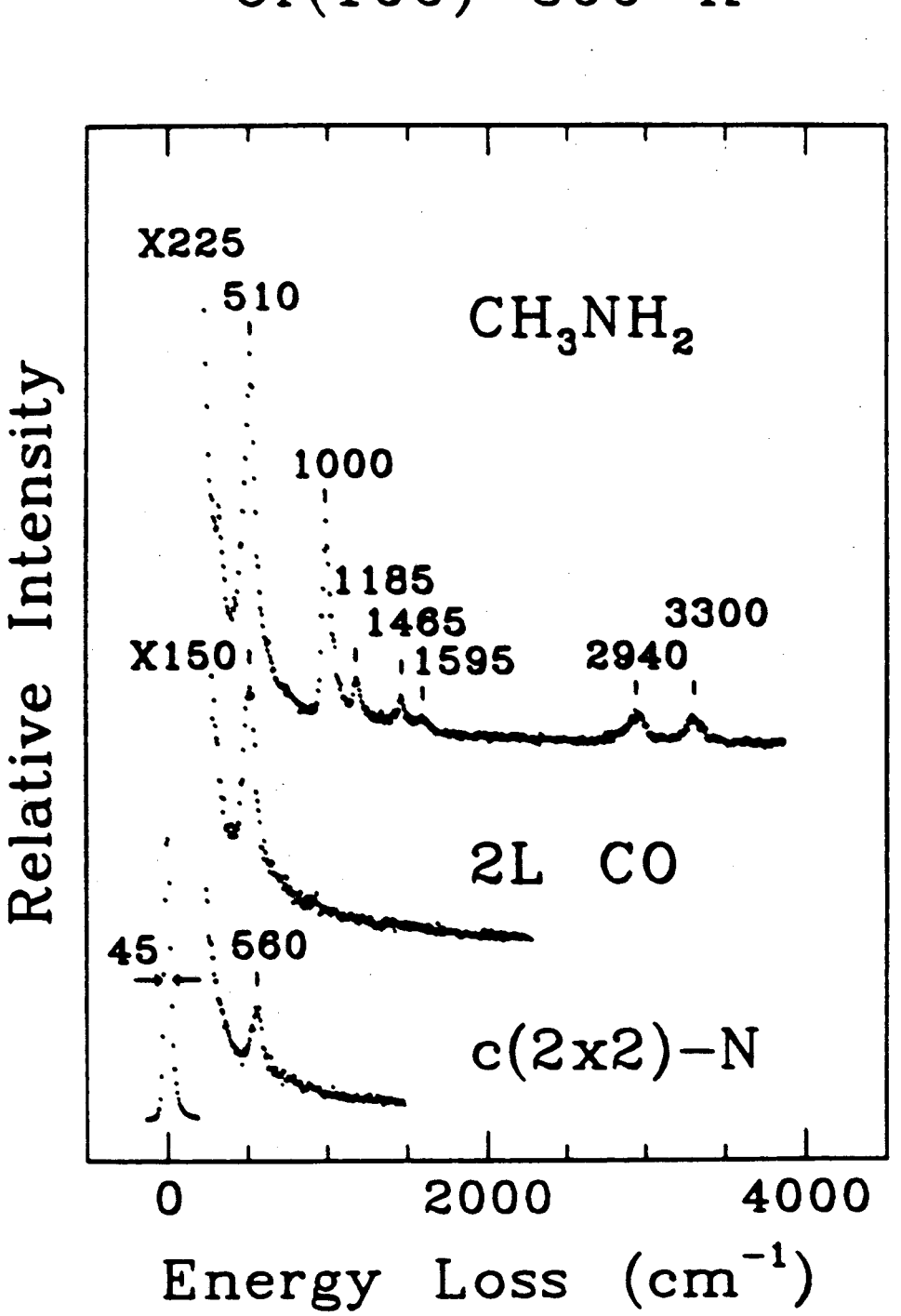

XBL 8412-5209

Figure 3

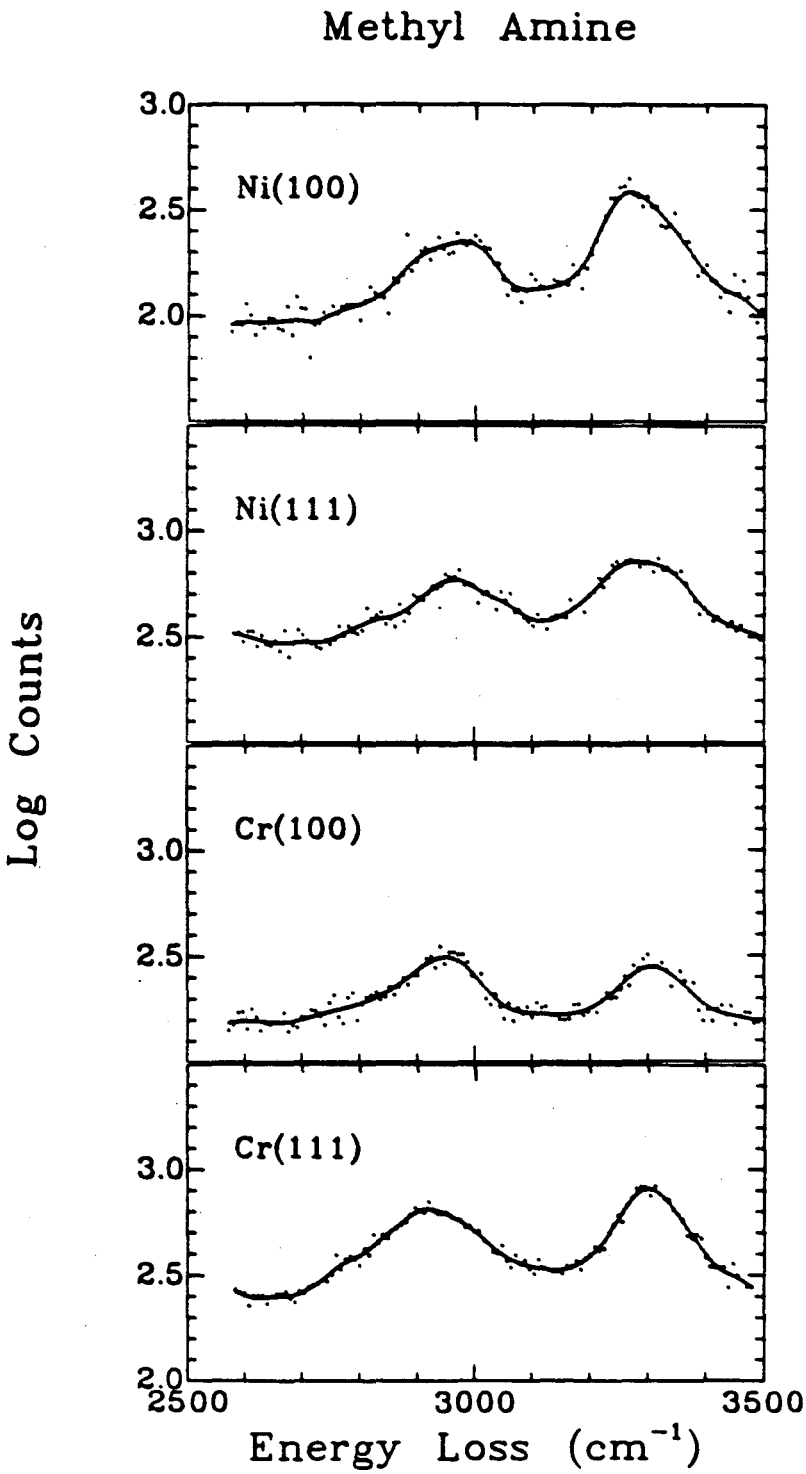
Methyl Amine
Ni(100)
Ni(111)
Cr(100)
Cr(111)
3.0
2.5
2.0
Log Counts
2500
3000
3500
Energy Loss (cm^{-1})
XBL 851-1060

Figure 4

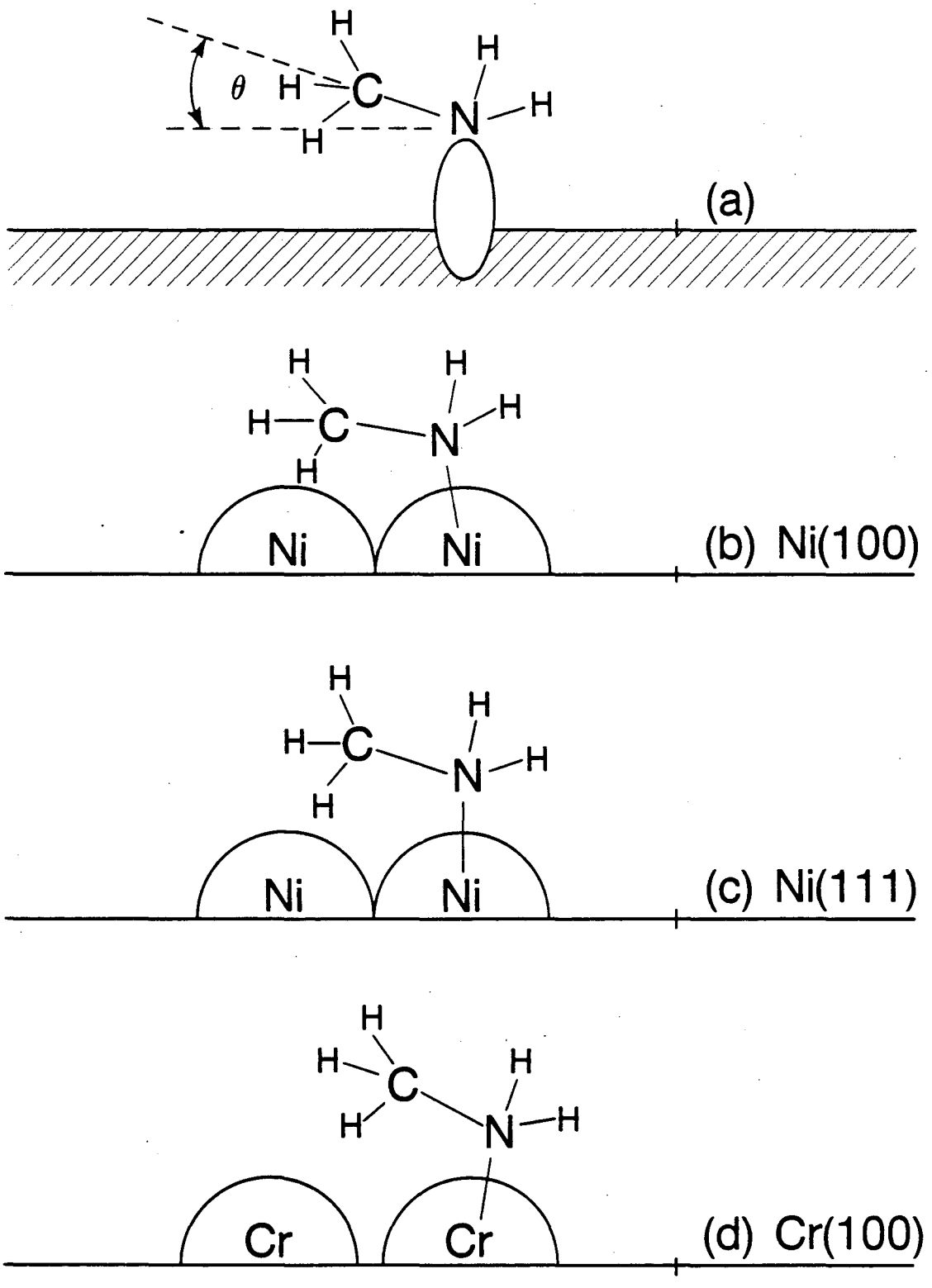

XBL 8412-5383

Figure 5

CH_3NH_2: Ni(100), Ni(111)

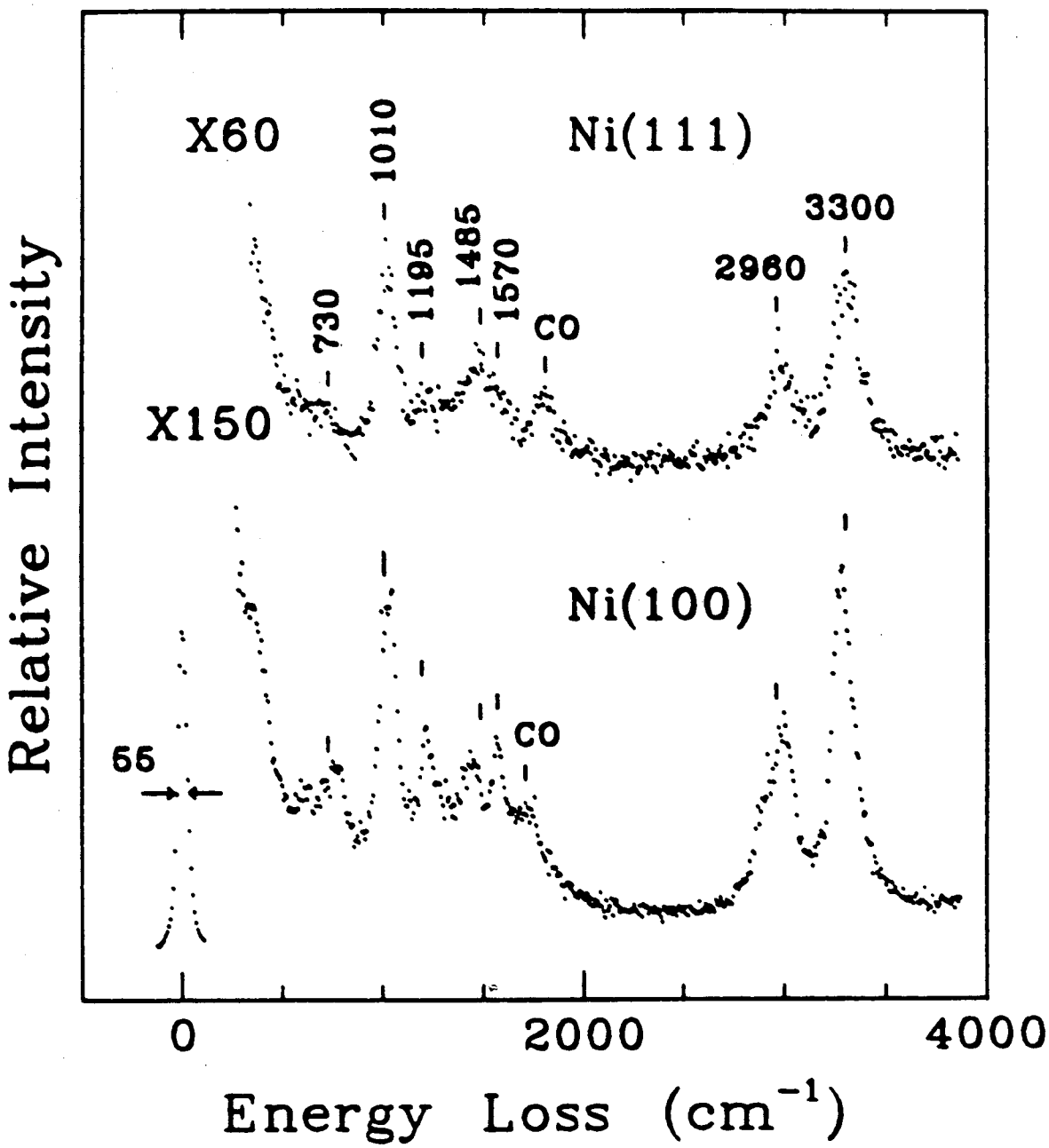

XBL 8412-5207

Figure 6

This report was done with support from the Department of Energy. Any conclusions or opinions expressed in this report represent solely those of the author(s) and not necessarily those of The Regents of the University of California, the Lawrence Berkeley Laboratory or the Department of Energy.

Reference to a company or product name does not imply approval or recommendation of the product by the University of California or the U.S. Department of Energy to the exclusion of others that may be suitable.

TECHNICAL INFORMATION DEPARTMENT
LAWRENCE BERKELEY LABORATORY
UNIVERSITY OF CALIFORNIA
BERKELEY, CALIFORNIA 94720